Design of a Coplanar-Waveguide-Based Microwave-to-Spin-Wave Transducer

Hadrian Renaldo O. Aquino[1], David Connelly[1], Alexei Orlov[1], Jonathan Chisum[1], *Senior Member, IEEE*, Gary H. Bernstein[1], *Fellow, IEEE*, and Wolfgang Porod[1], *Fellow, IEEE*

[1]Department of Electrical Engineering, University of Notre Dame, Notre Dame, IN 46556, USA

Spin waves are an emerging alternative to electrical signals for high-speed computing. One approach to realizing spin-wave computing devices is to make use of the diffraction and interference of spin waves in a magnetic thin film. This new class of device requires spin wave transducers that operate across a relatively wide bandwidth. Coplanar-waveguide-based transducers would typically be unsuitable for this application due to their comb-like frequency response. Our simulations show that if the coplanar waveguide is placed to the side of the edge of a magnetic film, the frequency response is greatly improved at the expense of peak transducer efficiency. We also found that the coplanar waveguide on top of the film with an etched gap in the film to the side of the waveguide can be a more efficient transducer for shorter decay lengths.

***Index Terms*—Magnonics, spin waves, microwave magnetics, micromagnetics.**

I. Introduction

Due to their relatively short wavelengths at microwave frequencies, spin waves are emerging as a potential alternative to electrical signals for high-speed computing and information processing [1], [2]. This work is part of an effort to design and fabricate a spin-wave-based real-time spectrum analyzer that exploits spin-wave interference by analogy to an optical spectrometer [3], [4]. In this new class of device, millimeter or microwave electrical signals are converted into spin waves with micrometer wavelengths. All processing is then done by the diffraction and interference of spin waves as they propagate in a magnetic thin film. After the interference pattern forms, spin waves are then converted back into electrical signals.

This type of device requires spin waves with isotropic dispersion relations, which, in turn, requires DC bias fields perpendicular to the plane of the magnetic film. These spin waves are forward-volume spin waves (FVSW) [5], [6]. The focus of the work presented here is to explore the design space of a microwave-to-spin-wave transducer for FVSWs, where the microwave signal is introduced by a coplanar waveguide (CPW).

Using CPWs as an inductive antenna to launch spin waves in a magnetic film has been demonstrated [7]-[9]. Compared to striplines or microstrips, CPWs have the benefit of being easy to fabricate and to integrate with on-chip RF circuits due to the need for only one layer of metallization. However, CPW-based spin-wave transducers would normally have spin-wave excitation spectra that would not be appropriate for our target application. This work demonstrates that an inductive antenna on the edge of a magnetic film can launch spin waves over a relatively wide frequency range.

Consider a magnetic thin film that is in the presence of a sufficiently high, DC bias magnetic field and an RF magnetic field with a frequency higher than the resonance frequency of the film. Typically, every point in a magnetic film excited by the external RF field launches a spin wave. The observable, total spin wave is then the result of the interference between all the excited spin waves whose amplitudes depend on the strength of the field acting on the launching point of the spin wave and their phase differences, which depend on the relative location of their launching points. The spin wave excitation spectrum of the RF field is then equivalent to the Fourier transform (FT) of the spatial distribution of the magnetic field that acts on the magnetic film [6], [10].

If the magnetic field is due to currents on a CPW that resides on the surface of the film, this interference results in a comb-like frequency response. However, because the spectrometer described above requires a relatively constant transfer function over the full bandwidth, i.e., without nulls, the comb-like excitation spectrum from a CPW would not be suitable for our applications.

Now consider a CPW that is not on, but is located close to the edge of the film. Launching spin waves from the edge of the film can be used to improve the spin-wave excitation spectrum. First, it has been shown that the edge of a film can be an efficient broadband source of spin-waves due to a gradient in the local ferromagnetic resonance frequency caused by the changing effective field near the edge of a magnetic film [11], [12]. Second, only part of the CPW's field acts on the magnetic film and can now be thought of roughly as a delta function. The FT of only that part describes the excitation spectrum; the FT of this spatial distribution is more broadband than that of the previous case where the CPW is on the film.

II. Methods

To design the edge-launched spin-wave transducer, micromagnetic simulations were done in Mumax3 [13]. The cells have in-plane dimensions of 10 nm × 10 nm. The simulation areas are 8-cell-wide strips with repeating periodic boundary conditions of 4096 repetitions along the width of the strip. The magnetic field used was taken from gold CPWs on gadolinium gallium garnet substrates simulated in Ansys HFSS with a voltage of 1V. The field has a peak in-plane component $H_x = 3.1$ mT and out-of-plane component $H_z = 4.6$ mT at 50 nm below the outer edge of the ground lines.

Reflections from the ends of the strips were minimized by slowly increasing the damping parameter, α, of the Landau-Lifshitz equation in a parabolic profile [14]. α increases from the bulk value to α = 1 over 32 μm at the outer edge of the simulation space opposite the launch edge.

The in-plane magnetization of the spin waves were fit to $M_x(x) = Ae^{-x/l_d}\sin(kx + \phi)$, where x is the distance from either the edge of the CPW or the edge of the magnetic film, l_d is the decay length, ϕ is the phase, and k is the wavenumber. The starting amplitude, A, is compared between different wavenumbers to show the response of the transducer.

III. Results and Discussion

A. CPW on top of the film

As mentioned above, a CPW placed on a magnetic film, as shown in Fig. 1(a), exhibits a comb-like frequency response. However, if the amplitude of the RF field is large such that the precession angle of the local magnetizations is large, nonlinear effects become significant, which results in significantly varying spatial frequencies and unwanted additional frequency components. The structure shown on Fig. 1(a) is simulated, and a resulting spin wave with nonlinear effects is shown in Fig. 1(b). This plot shows the component of the magnetization along the x axis (M_x). The center of the CPW is at $x = 0$. The magnetic parameters of a typical yttrium iron garnet (YIG) film are used: saturation magnetization M_S = 140 kA/m, $\alpha = 2 \times 10^{-4}$and thickness t = 100 nm. These are typical values for YIG films as reported in [15]. YIG was chosen because of its extensive use in magnonics due to its extremely low damping. An external DC bias of 300 mT was used and the RF field has a frequency of 3.72 GHz, which results in k = 2.2 rad/μm. The field is taken from an HFSS simulation of a CPW with 2 μm wide signal and ground lines that are 300 nm thick and 2 μm apart and on a gadolinium gallium garnet (GGG) substrate. These dimensions were arbitrarily chosen as representative of CPWs in the frequency range of interest. A representative schematic is shown in Fig. 1.

FIG. 1 HERE

If the field is reduced, so do the nonlinear effects. Shown in Fig. 1(c) is a plot of M_x of a spin wave under the same conditions and material parameters as in Fig. 1(b) but for a magnetic field strength that is 1/100 smaller. This results in a spin wave having essentially one temporal frequency at a near constant wavelength, and hence, wavenumber.

The starting amplitude, A, of the spin wave is, in this case, defined as the amplitude at x = 5 μm, which is at the outer edge of the CPW. Fig. 1(c) is an example of a spin wave having a starting amplitude of about 1.9 kA/m. Sweeping the frequency and fitting M_x as described in Section II yields a plot of the starting A for various wavenumbers. Fig. 2(a) shows the same structure, but now along with the FT of the applied field, shown in Fig. 2(b). The starting amplitude as a function of wavenumber, indicated by the asterisk symbols, shows good agreement with the FT of the applied field.

FIG. 2 HERE

B. CPW to the side of the film

As mentioned previously, the film edge can be used to broaden the spin-wave excitation spectrum. The edge of a film can be an efficient broadband source of spin-waves, only part of the CPW's field acts on the film, and the FT of only that part describes the excitation spectrum, which is now no longer comb-like. The frequency response of the raised CPW is shown by the circles in Fig. 2(b) and does not show any nulls. This improved bandwidth comes at the cost of transducer efficiency since only the field to the side of the CPW acts on the magnetic film.

Because the magnetic field varies spatially, the position of the CPW relative to the edge of the film becomes an important design parameter in optimizing transducer efficiency. The CPW and its edge where the film is to be located is shown in Fig. 3(a), and the magnitude of the magnetic field just past the outer edge of the CPW is shown in Fig. 3(b). The metal shown in Fig. 3(a) is located vertically between 0 and 0.2 μm in Figs. 3(b) and 3(c). Fig. 3(b) shows that the magnetic field is strongest just along the edge of the metal.

FIG. 3 HERE

However, it is not the magnitude of the field, but rather the in-plane component of the field, that drives the spin waves. Looking at the location of the strongest field in 3(b), we might intuitively conclude that the film should be located here. Because the focus of this work is launching FVSWs, an additional consideration must be made. Because the out-of-plane component of the RF field is parallel to the DC bias field, it contributes very little to the excitation of spin waves. Fig. 3(c) reveals that the in-plane component is strongest just above and below the metal line; we find that placing the CPW raised up (by placing it on a non-magnetic, non-conducting layer) such that the bottom of the CPW is in the same plane as the top of the magnetic film (as shown in Fig. 4a, structure 1) would have a much stronger in-plane field acting on the edge of the film as compared to if the bottom of the CPW were at the same plane as the bottom of the film (as shown in Fig 4a, structure 2). Fig. 4b shows simulations comparing these configurations (and others) for a magnetic film with t = 243 nm M_S = 140 kA/m and $\alpha = 4 \times 10^{-3}$ with an external DC bias of 196 mT.

FIG. 4 HERE

C. Using stray fields

A third and fourth configuration considered places the CPW on the magnetic film (Figs. 4(a) structures 3 and 4) and includes a gap in the film to the side of the CPW [16]. The left side of the gap is where the transducer is located and the right side is where the spin-wave device (i.e., spectrometer) is located. The extended film with a gap accomplishes two things: it moves the CPW far from the active spin-wave launch site so that its field is less significant, and it couples the spin-wave field in the transducer film (left side) across the gap. As a result, the film to the left of the gap is nearly solely responsible for launching the spin wave in the active area of the device.

As shown in Fig. 1(b), large fields cause magnon-magnon interactions [17]-[19], which are highly nonlinear and produce unwanted additional frequency components. The gap may be chosen to attenuate the undesired frequency components, leaving only the frequency of the RF signal, thus launching a spin wave at only the desired frequency.

The simulation results of Fig. 4(b) compare the resulting spin waves for all four configurations, structures 1 – 4. When the gap is moved from the edge of the CPW (structure 3) to 6 μm from the CPW (structure 4), the amplitude of the resulting spin wave is larger than that without the material under the CPW (structure 1), and is the largest of all the configurations.

Care must be taken when using this structure to launch spin waves because the undesired frequency components can launch spin waves across the gap. Using the same magnetic parameters as in Section III.A for YIG (M_S = 140 kA/m, $\alpha = 2 \times 10^{-4}$ and thickness t = 100 nm) and with a DC bias of 300 mT and an RF field at 3.72 GHz, the simulation results in a wave with significant pollution in its spectrum as shown in Fig. 5(a).

FIG. 5 HERE

If the field of the structure-4 configuration is increased to 500 mT and the gap placed 15 μm away from the outer edge of the CPW, the simulation results in a spin wave of a single frequency as shown in Fig. 5(b). We conjecture that this filtering of the undesired frequency components is due to a decrease in the decay length of the spin waves associated with the magnon-magnon interactions in the larger DC bias. This filtering was also observed when the field was kept constant, but the decay length was decreased by increasing the damping such as the films in Fig. 4.

The efficiency of this structure depends on the thickness of the magnetic film. For the 100 nm films in Fig. 5, we found this structure produces lower-amplitude spin waves when compared to the structure in structure 4 of Fig. 4 (t = 243 nm).

Simulations were performed assuming a 300 nm thick film with M_S = 112 kA/m and $\alpha = 4 \times 10^{-3}$ with a DC bias of 160 mT. The frequency of the RF field was swept to extract the frequency response of the transducers and is shown in Fig. 6. The results of two transducers are shown. First, the CPW is raised and to the side of the film 2 μm away. Second, a transducer with a 2 μm gap is to the side of the CPW. Both configurations show a frequency response without nulls. However, because the distance between the CPW and the edge is larger than in Fig. 2, the amplitude of the spin wave from the first configuration of Fig. 6 is much lower. This demonstrates that the field that launches the spin wave across the gap is mostly the stray field from the material under the CPW.

FIG. 6 HERE

IV. Summary and Conclusion

Using a CPW would usually be a poor choice for launching spin waves over a relatively wide bandwidth due to the presence of nulls in the spin wave excitation spectra. However, placing the CPW to the side of the edge of the magnetic thin film produces a frequency response without nulls at the expense of peak transducer efficiency. To maximize the amplitude of the spin wave launched, the CPW should be raised such that the bottom of the CPW is in-plane with the top of the magnetic film rather than directly on the substrate.

We have also found that under certain conditions, placing the CPW on the magnetic film and creating an edge by etching a gap in the magnetic material to the side to the CPW can be a more-efficient transducer. Rather than the field from the CPW, the field that contributes most is the stray field from the magnetic material under the CPW. Careful design of this type of transducer is necessary, however, to avoid the presence of unwanted additional frequency components in the launched spin wave.

Acknowledgment

This work was supported by the National Science Foundation (NSF) through the Spectrum Efficiency, Energy Efficiency, and Security (SpecEES) program.

References

[1] G. Csaba, Á. Papp and W. Porod, "Perspectives of using spin waves for computing and signal processing," Physics Letters A, vol. 381, no. 17, pp. 1471-1476, 2017.

[2] G. Csaba, A. Papp and W. Porod, "Spin-wave based realization of optical computing primitives," Journal of Applied Physics, vol. 115, no. 17, pp. 17C741, 2014.

[3] Á. Papp, W. Porod, Á. Csurgay and G. Csaba, "Nanoscale spectrum analyzer based on spin-wave interference," Scientific Reports, vol. 7, no. 1, 2017.

[4] H. Aquino et al., "Towards a Chip-Scale Millimeter-Wave Spectrum/Signal Analyzer Using Spin-Wave Diffraction and Interference," 2020 IEEE Silicon Nanoelectronics Workshop (SNW), Honolulu, HI, USA, 2020, pp. 127-128.

[5] S. Klingler, P. Pirro, T. Brächer, B. Leven, B. Hillebrands and A. Chumak, "Spin-wave logic devices based on isotropic forward volume magnetostatic waves," Applied Physics Letters, vol. 106, no. 21, p. 212406, 2015.

[6] J. Chen et al., "Spin wave propagation in perpendicularly magnetized nm-thick yttrium iron garnet films," Journal of Magnetism and Magnetic Materials, vol. 450, pp. 3-6, 2018.

[7] V. Kruglyak, S. Demokritov and D. Grundler, "Magnonics," Journal of Physics D: Applied Physics, vol. 43, no. 26, p. 264001, 2010.

[8] M. Bailleul, D. Olligs and C. Fermon, "Propagating spin wave spectroscopy in a permalloy film: A quantitative analysis," Applied Physics Letters, vol. 83, no. 5, pp. 972-974, 2003.
[9] A. Papp, G. Csaba, H. Dey, M. Madami, W. Porod and G. Carlotti, "Waveguides as sources of short-wavelength spin waves for low-energy ICT applications," The European Physical Journal B, vol. 91, p. 107, 2018.
[10] S. Maendl, I. Stasinopoulos and D. Grundler, "Spin waves with large decay length and few 100 nm wavelengths in thin yttrium iron garnet grown at the wafer scale," Applied Physics Letters, vol. 111, no. 1, p. 012403, 2017.
[11] F. Mushenok, R. Dost, C. Davies, D. Allwood, B. Inkson, G. Hrkac and V. Kruglyak, "Broadband conversion of microwaves into propagating spin waves in patterned magnetic structures," Applied Physics Letters, vol. 111, no. 4, p. 042404, 2017.
[12] C. Davies, V. Poimanov and V. Kruglyak, "Mapping the magnonic landscape in patterned magnetic structures," Physical Review B, vol. 96, no. 9, p. 094430, 2017.
[13] A. Vansteenkiste, J. Leliaert, M. Dvornik, M. Helsen, F. Garcia-Sanchez and B. Van Waeyenberge, "The design and verification of MuMax3," AIP Advances, vol. 4, no. 10, p. 107133, 2014.
[14] G. Venkat, H. Fangohr and A. Prabhakar, "Absorbing boundary layers for spin wave micromagnetics," Journal of Magnetism and Magnetic Materials, vol. 450, pp. 34-39, 2018.
[15] A. Chumak, A. Serga and B. Hillebrands, "Magnonic crystals for data processing," Journal of Physics D: Applied Physics, vol. 50, no. 24, p. 244001, 2017.
[16] H. Aquino, D. Connelly, A. Orlov, J. Chisum, G. H. Bernstein and W. Porod, "Using Coplanar Waveguides as Spin-Wave Sources with Improved Bandwidth," 2020 Device Research Conference (DRC), Columbus, OH, USA, 2020, pp. 1-2.
[17] H. Suhl, "The theory of ferromagnetic resonance at high signal powers," Journal of Physics and Chemistry of Solids, vol. 1, no. 4, pp. 209-227, 1957.
[18] E. Schlömann, "Fine Structure in the Decline of the Ferromagnetic Resonance Absorption with Increasing Power Level," Physical Review, vol. 116, no. 4, pp. 828-837, 1959.
[19] S. Rezende and F. de Aguiar, "Spin-wave instabilities, auto-oscillations, and chaos in yttrium-iron-garnet," Proceedings of the IEEE, vol. 78, no. 6, pp. 893-908, 1990.

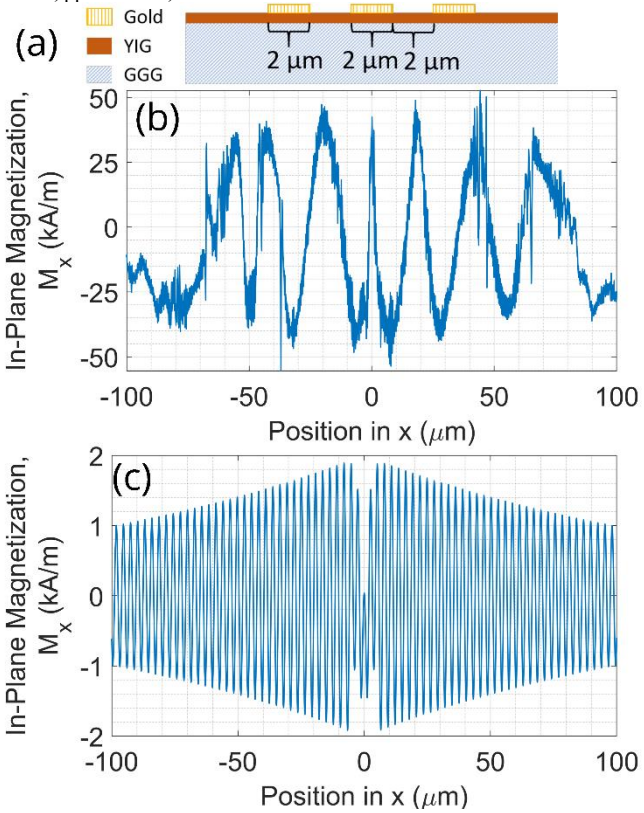

Fig.1. Simulation results showing large-amplitude spin waves with significant nonlinear effects and a spin wave without significant nonlinear effects. (a) Cross section of the structure simulated in (b) and (c) showing a CPW on a magnetic film. (b) In-plane magnetization in a magnetic film resulting from launching large amplitude spin waves. The center of the CPW is at $x = 0$. (c) In-plane magnetization of a spin wave launched with 1/100th magnitude of magnetic field. In both (b) and (c) the RF field has a frequency of 3.72 GHZ and the bias field is 300 mT. The magnetic film has $M_S = 140$ kA/m and $\alpha = 2 \times 10^{-4}$ and a thickness of 100 nm.

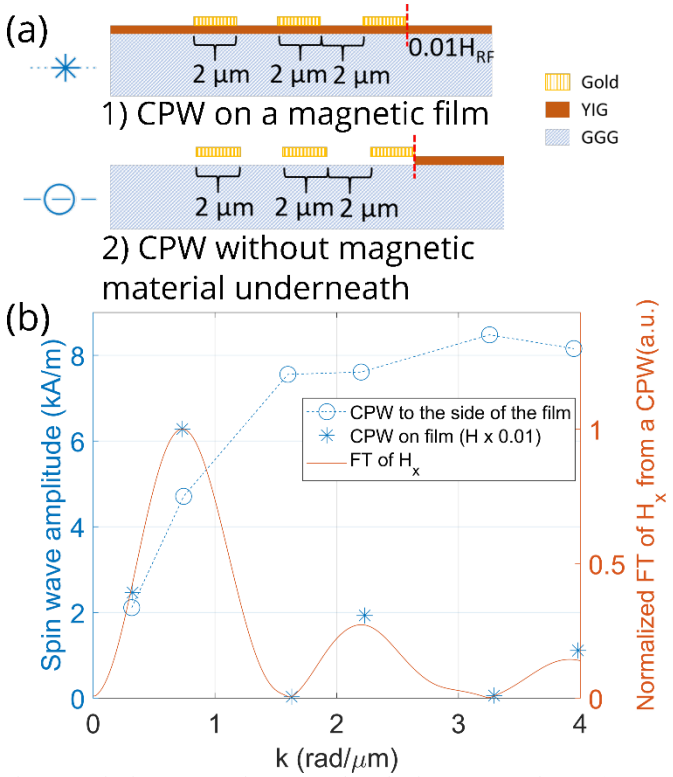

Fig. 2. Excitation spectra of two CPW-based spin-wave transducers. (a) Cross sections of the structures simulated. The vertical red lines indicate the locations of the starting amplitudes. 1) The CPW is placed on the film with a field 1/100th of (2); 2) The CPW is placed on a non-magnetic, non-conducting layer to the side of the film. (b) Excitation spectra of two CPW-based spin wave transducers. Also shown is the FT of the field from the CPW which shows good agreement with the frequency response of the transducer with the CPW on the film.

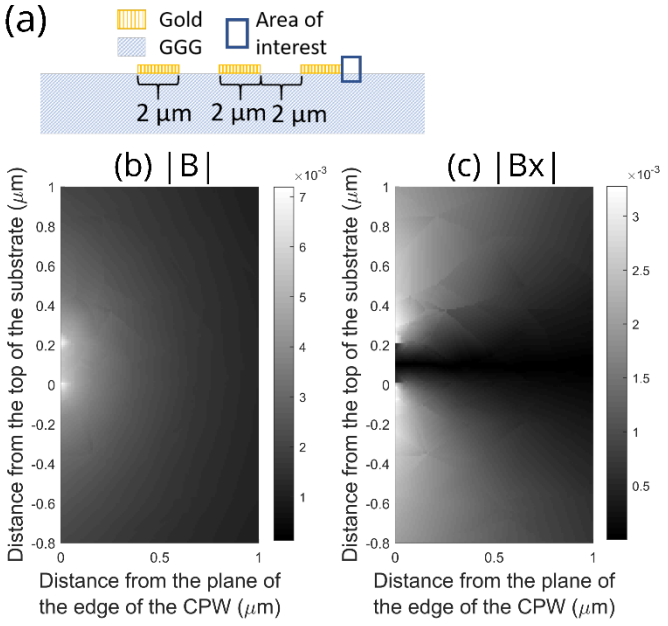

Fig. 3. The B field from a CPW. (a) Cross section of waveguide showing area of interest to the right (square) where magnetic field is shown in (b) and (c). The bottom of the CPW is at y = 0 and is 200 nm thick. (b) The magnitude of

the B field (T) from the CPW. (c) Magnitude of the in-plane component of the B field (T) from the CPW.

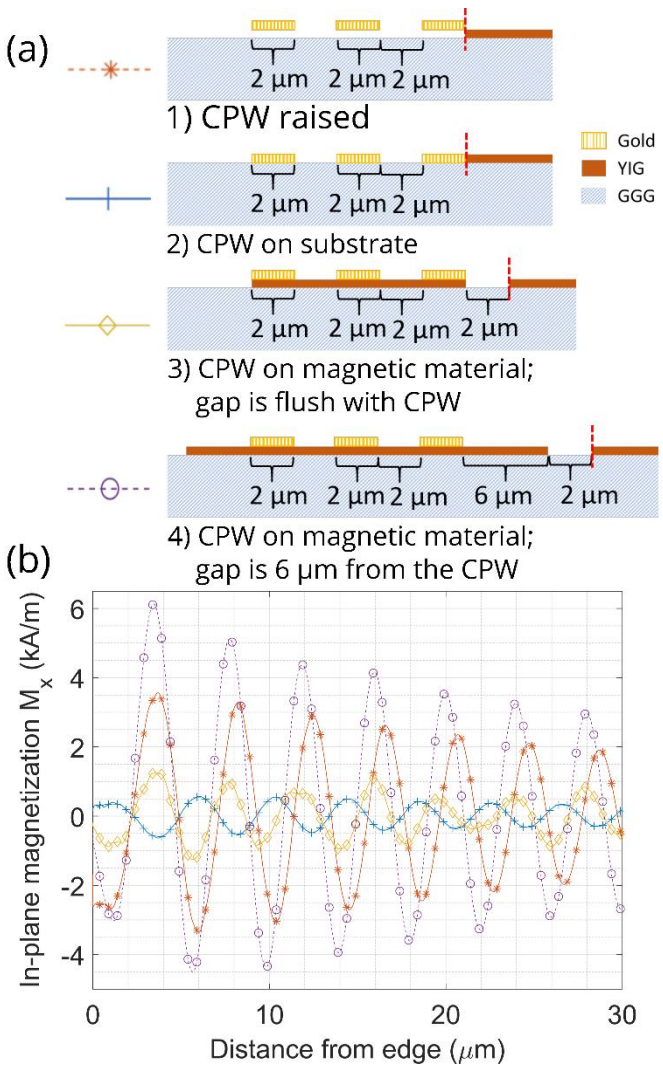

Fig. 4. Four possible launcher configurations and their resulting spin waves. (a) Cross sections of the structures. The vertical red lines indicate the locations of the starting amplitudes. 1) The edge is flush to the CPW and the bottom of the 300 nm thick CPW is in the same plane as the bottom of the magnetic film; 2) the CPW on top of the substrate; 3) the CPW is on the magnetic film with a 2 μm gap etched to the side of the CPW; and 4) the CPW is on the magnetic film with the gap 6 μm to the side. (b) Spin waves launched from the edge of a 243 nm thick YIG film with M_S = 140 kA/m, $\alpha = 4 \times 10^{-3}$ with an external DC bias of 196 mT. All plots begin at the edge of the magnetic film. The markers correspond to the associated structures in part (a).

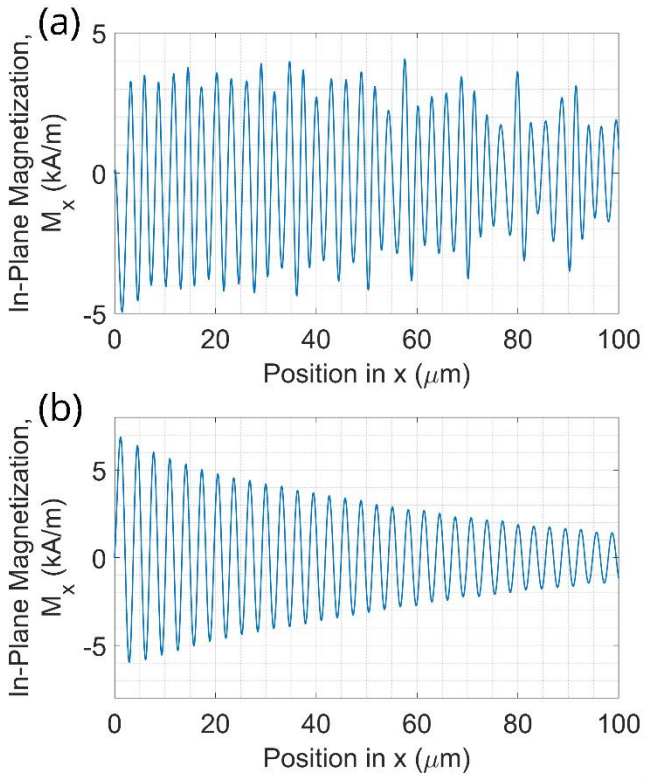

Fig. 5. Spin waves launched from the edge of a 100 nm thick magnetic film with M_S = 140 kA/m and $\alpha = 2 \times 10^{-4}$ with DC bias fields of (a) 300 mT and (b) 500 mT.

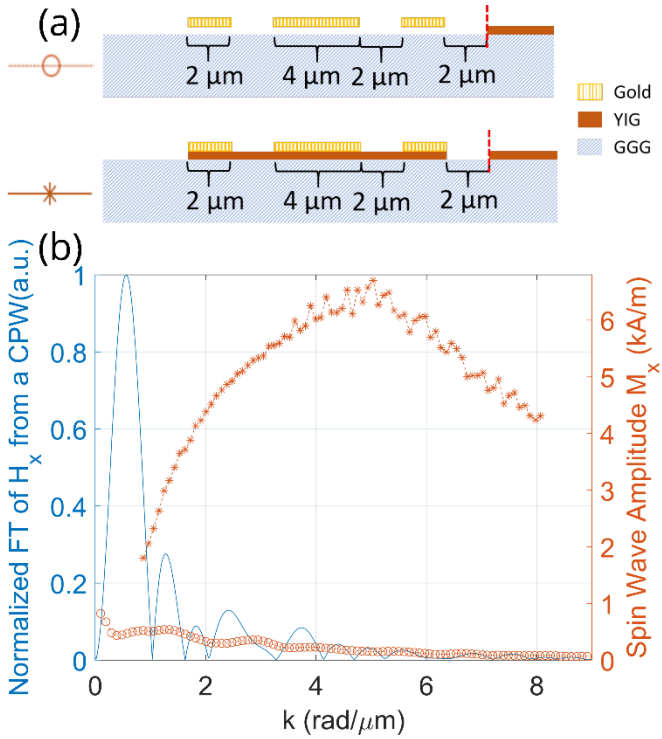

Fig. 6. Excitation spectra of two CPW-based spin-wave transducers. a) Cross sections of the structures simulated. The vertical red lines indicate the locations of the starting amplitudes. 1) The CPW is raised and to the side of the film 2 μm away; 2) the CPW is placed on the film with a 2 μm gap to the side; (b) FT of the RF magnetic field from the CPW (solid line), spin-wave amplitude as a function of k for structure 1 (circle markers), and spin-wave amplitude as a function of k for structure 2 (asterisk markers). Both configurations show a frequency response without nulls.